Effect of Ion-Binding and Chemical Phospholipid Structure on the Nanomechanics of Lipid Bilayers Studied by Force Spectroscopy

Sergi Garcia-Manyes, Gerard Oncins, and Fausto Sanz
Department of Physical Chemistry, Universitat de Barcelona, Barcelona, Spain

ABSTRACT The nanomechanical response of supported lipid bilayers has been studied by force spectroscopy with atomic force microscopy. We have experimentally proved that the amount of ions present in the measuring system has a strong effect on the force needed to puncture a 1,2-dimyristoyl-*sn*-glycero-3-phosphocholine bilayer with an atomic force microscope tip, thus highlighting the role that monovalent cations (so far underestimated, e.g., Na^+) play upon membrane stability. The increase in the yield threshold force has been related to the increase in lateral interactions (higher phospholipid-phospholipid interaction, decrease in area per lipid) promoted by ions bound into the membrane. The same tendency has also been observed for other phosphatidylcholine bilayers, namely, 2-dilauroyl-*sn*-glycero-3-phosphocholine, 1,2-dipalmitoyl-*sn*-glycero-3-phosphocholine, and 1,2-dioleoyl-*sn*-3-phosphocholine, and also for phosphatidylethanolamine bilayers such as 1-palmitoyl-2-oleoyl-*sn*-3-phosphoethanolamine. Finally, this effect has been also tested on a natural lipid bilayer (*Escherichia coli* lipid extract), showing the same overall tendency. The kinetics of the process has also been studied, together with the role of water upon membrane stability and its effect on membrane nanomechanics. Finally, the effect of the chemical structure of the phospholipid molecule on the nanomechanical response of the membrane has also been discussed.

INTRODUCTION

The physical and chemical properties of biological membranes are crucial to understanding membrane functions. The main biological role of bilayers is to provide a barrier that divides electrolytic solutions into different compartments. Therefore, the effect of electrolytic solutions on membranes is of great importance and has generated wide research (1). Besides, ion binding affects the stability of proteins and their process of binding to membranes (2), and it is also mainly responsible for lipid vesicle fusion (3,4).

From an experimental point of view, many works, especially in the 1980s, have dealt with the quantification of membrane surface potential through the electrophoretic mobility of lipid membranes under solutions with different ionic strength, allowing the calculation of the ζ-potential value (5,6). More recently, contributions regarding infrared (2) and fluorescent techniques have also helped to shed light on this issue. Finally, recent molecular dynamics (MD) simulations have allowed us to understand the underlying processes from an atomistic point of view and have helped us to study the role that cations play upon membrane structure and stability (7–9). Between the experimental macroscopic techniques and the theoretical atomistic approaches to this issue, atomic force microscopy (AFM) has proved to be a powerful technique that has allowed imaging of surfaces with subnanometric resolution. This technique has helped us to understand how supported planar lipid bilayers (SPBs) assemble and what the interaction forces are that act between vesicle and substrate surfaces and also between membrane surfaces, which is fundamental to efforts in chemistry, structural biology, and biophysics (10,11).

SPBs have been used as model membranes to study cell-cell recognition in the immune system, adhesion of cells, phospholipid diffusion, protein binding to lipid ligands, and membrane insertion of proteins (12,13). By imaging lipid bilayers in aqueous media with AFM, both molecular structure and morphological aspects have been demonstrated (14–17). Besides, the force spectroscopy mode allows us to obtain valuable experimental information about the mechanics of the systems with nanometric and nanonewton resolution. In recent years, force spectroscopy has been applied to the study of nanomechanical properties of different systems including nanoindenting hard surfaces (18,19) or cells (20), studying the solvation forces near the surfaces (21,22), dealing with the interactions of chemically functionalized probes and surfaces (so-called chemical force microscopy) (23,24), or unfolding protein molecules (25,26). Thanks to these force measurements, valuable information can be obtained regarding phospholipid interaction forces such as those generated by either Derjaguin-Landau-Verwey-Overbeek (DLVO) forces, hydration forces, or steric forces (27). Recent contributions have dealt with membrane nanomechanics using force spectroscopy, especially regarding measurement of the elastic/plastic behavior of the bilayer as a function of its composition, or the interaction with chemically modified probes (16,27,28).

Concerning the force curves on lipid bilayers, some authors have described jumps on the approaching curve, this breakthrough being interpreted as the penetration of the AFM tip through the lipid bilayer (29). The force at which this jump in the force plot occurs is the maximum force the bilayer is able to withstand before breaking. Therefore,

Submitted April 5, 2005, and accepted for publication June 7, 2005.

Address reprint requests to Fausto Sanz, Dept. of Physical Chemistry, Universitat de Barcelona, 1-11 Martí i Franquès, 08028 Barcelona, Spain. Tel.: 34-934021240; Fax: 34-934021231; E-mail: fsanz@ub.edu.

0006-3495/05/09/1812/15 $2.00

doi: 10.1529/biophysj.105.064030

a quantitative measurement of the force at which the jump occurs can shed light on basic information concerning cell membrane nanomechanics as well as interaction forces between neighboring lipid molecules in the membrane. Some of the factors (variables) involved in membrane stability can be assessed through this jump in the force plot thanks to those force spectroscopy measurements. Likewise, the force at which this jump occurs can be regarded as a ''fingerprint'' of the bilayer stability under the experimental conditions in which the measurement is performed, just as force is the fingerprint for a protein to unfold or for a hard material surface to be indented. Controlling the involved variables can result in a better understanding of the regulating processes that nature can use to govern cell membrane interactions.

So far, the main reported variables for breakthrough dependence are 1), temperature (phase); 2), tip chemistry and phospholipid chemistry; and 3), tip approaching velocity. Concerning temperature, although there is much debate about whether the jump can be observed in both the gel and liquid phases or only in the gel phase, little is known experimentally about this dependence except for a report in a recent publication (30) in which it is posited that the breakthrough force decreases as the temperature increases. Regarding tip chemistry and phospholipid chemistry, it has been demonstrated that although hydrophilic tips yield a high material-dependent breakthrough force, hydrophobic tips give rise to a breakthrough force near the contact force (28). Finally, the greater the tip approaching velocity, the higher the force at which the jump will occur (31,32). However, even though those parameters are now being studied, there are two fundamental issues that have not yet been elucidated: 1), the effect of phospholipid chemical structure; and 2), the effect of the ionic strength of the measuring media on the yield threshold value. Regarding the former, a first approach has been reported (27,28), but there are still some questions lacking answers: Is the polar head in the phospholipid molecule the element mainly responsible for the bilayer nanomechanics or does the hydrophobic tail also play an important role? And further, does the degree of insaturation also play a role in the compactness of the bilayer?

Concerning the issue of ionic strength, we know that electrostatic interactions govern structural and dynamical properties of many biological systems (33,34). In the case of phospholipid bilayers, the role of monovalent ions (e.g., Na^+) seems to have been so far underestimated, as theoretical simulations seem to predict. Indeed, MD simulations (9,35) suggest a strong interaction between sodium and calcium ions and the carbonyl oxygens of the lipids, which thus forms tight ion-lipid complexes, giving rise to a higher degree of membrane organization. Likewise, the lateral interaction between the phospholipid molecules increases, with the overall result of a more efficient packing (reduction of the area per lipid value) of the phospholipid structure. Since natural lipid membranes are composed of different phospholipid molecules in a wide range of concentrations, it is always difficult to assess the contribution of every type of phospholipid to the total nanomechanical response of the system. The role of ionic strength can be tested on all phospholipid systems, even though for the sake of simplicity, and to start with, we first dealt with model lipid membranes such as 1,2-dimyristoyl-*sn*-glycero-3-phosphatidylcholine (DMPC), 1,2-dilauroyl-*sn*-glycero-3-phosphocholine (DLPC), and 1,2-dipalmitoyl-*sn*-glycero-3-phosphocholine (DPPC) deposited on mica. Later on, the study was extended to a phosphatidylethanolamine (PE) bilayer, and finally, the nanomechanical response of a natural lipid bilayer (*Escherichia coli* lipid extract) was studied.

The goal of this study is mainly to demonstrate an experimental, quantitative force spectroscopy detailed approach to understanding the nanomechanics of lipid bilayers and the forces involved in membrane deformation and failure in aqueous environment, especially dealing with the role of ionic strength on the nanomechanical response of the membrane. The discussion and interpretation of the results will be made in the framework of available data obtained through both theoretical calculations and experiments to correlate the changes in mechanical response of the system with the structural changes induced in the membrane upon ion binding considered from an atomic point of view. Additionally, we aim to perform a first approach to relate the chemical composition of the phospholipid molecule with its mechanical response.

MATERIALS AND METHODS

Sample preparation

DMPC (Sigma, St. Louis, MO) (>98%) was dissolved in chloroform/ethanol (3:1) (Carlo Erba, Milan, Italy; analysis grade 99.9%) to give a final DMPC concentration of 2 mM. This dissolution was kept at −10°C. A 500-μl aliquot was poured in a glass vial and the solvent was evaporated with a nitrogen flow, obtaining a DMPC film at the bottom of the vial. The solution was kept in a vacuum overnight to ensure the absence of organic solvent traces. Then, aqueous buffered solution at the correct ionic strength was added to achieve a final DMPC concentration of 500 μM containing 0 mM NaCl, 50 mM NaCl, 75 mM NaCl, 100 mM NaCl, and 150 mM NaCl + 20 mM $MgCl_2$, respectively. All solutions used in this work were set at pH 7.4 with 10 mM Hepes/NaOH. Because of the low solubility of DMPC in water, the vial was subjected to 30-s cycles of vortexing, temperature, and sonication until a homogeneous mixture was obtained. The solution was finally sonicated for 20 min (to have unilamellar liposomes) and allowed to settle overnight, always protected from light and maintained at 4°C. Before use, mica surfaces (Metafix, Madrid, Spain) were glued onto teflon discs with a water-insoluble mounting wax. Fifty microliters of DMPC dissolution at the specific NaCl concentration was applied to cover a 0.5-cm^2 freshly cleaved piece of mica for a deposition time of 35 min. After that, the mica was rinsed three times with 100 μl of the corresponding ionic aqueous solution. The process of vesicle formation and deposition for the rest of the phospholipid bilayers used in this work (DLPC, DPPC, 1-palmitoyl-2-oleoyl-*sn*-3-phosphoethanolamine (POPE), and 1,2-dioleoyl-*sn*-3-phosphocholine (DOPC), all from Sigma, >98%) is the same as that described for DMPC. In the case of DPPC, however, the temperature cycles for resuspension were set to ~50°C due to the higher T_m for this phospholipid. *E. coli* lipid extract (nominally 67% phosphatidylethanolamine, 23.2% phosphatidylglycerol, and 9.8% cardiolipin), was purchased from Avanti

Polar Lipids (Alabaster, AL). Basically, the polar lipid extract is the total lipid extract precipitated with acetone and then extracted with diethyl ether (36). The process for vesicle formation is also the same as the one described for DMPC.

ζ-Potential measurements

ζ-Potential measurements were performed with a Zetamaster Particle Electrophoresis Analyser through which the velocity of the particles can be measured with a light-scattering technique by using the Doppler effect thanks to a pair of mutually coherent laser beams (5 mW, He-Ne laser at 633 nm). Zetamaster measures the autocorrelation function of the scattered light and after the signal processing it obtains the electrophoretic mobility and, finally, through the Henry equation, the ζ-potential.

AFM imaging

AFM images were acquired with a Dimension 3100 (Digital Instruments, Santa Barbara, CA) microscope controlled by a Nanoscope IV controller (Digital Instruments) in contact mode using V-shaped Si_3N_4 cantilever tips (OMCL TR400PSA, Olympus, Tokyo, Japan). The applied force was controlled by acquiring force plots before and after every image was captured to measure the distance from the set point value.

Force spectroscopy

Force spectroscopy was performed with a Molecular Force Probe1-D, (Asylum Research, Santa Barbara, CA). Force plots were acquired using V-shaped Si_3N_4 tips (OMCL TR400PSA, Olympus) with a nominal spring constant of 0.08 N/m. Individual spring constants were calibrated using the equipartition theorem (thermal noise)(37) after having correctly measured the piezo sensitivity (V/nm) by measuring it at high voltages after several minutes of performing force plots to avoid hysteresis. It should be pointed out that the results shown here for DMPC bilayers were obtained with the same cantilever keeping the spot laser at the same position on the lever to avoid changes in the spring constant calculation (38). However, results have low scattering when using different tips and different samples; ~1300 curves over more than 15 positions were obtained for each sample. All force spectroscopy and AFM images were obtained at 20 $\pm$ 0.5°C, which is below the main phase transition temperature (T_m) of DMPC (23.5°C). Besides, we have to consider here that T_m for supported bilayers shifts to a higher temperature than observed in solution (39). Therefore, we are indenting the gel phase for DMPC supported bilayers. Applied forces F are given by $F = k_c \times \Delta$ where Δ is the cantilever deflection. The surface deformation is given as penetration (δ), evaluated as $\delta = z - \Delta$, where z represents the piezo-scanner displacement.

Chemically modified AFM probe preparation

Commercially available gold-coated cantilevers (OMCL-TR400PB, Olympus) with nominal spring constant of $k_c = 0.09$ N/m were cleaned and placed into a 10 mM 16-mercaptohexadecanoic acid (Sigma) isopropanol solution and kept at 4°C overnight. Before use, tips were rinsed with isopropanol and distilled water. Sonication was briefly applied to remove thiol aggregates that might be adsorbed. The quality of the self-assembled monolayers was confirmed using contact angle measurements.

RESULTS AND DISCUSSION

DMPC model membrane

A first experimental approach to study ion adsorption on the membrane is the measurement of the liposome mobility in an electrophoretic field and likewise measuring the ζ-potential. Although the ζ-potential does not directly yield the surface charge, but the charge at the point where the Stern layer and the diffuse layer meet (shear plane), it is considered to yield a significant approximation of the surface potential. Fig. 1 shows the evolution of the ζ-potential value of a DMPC unilamellar liposome solution as the ionic strength of the solution is increased. All concentrations refer only to NaCl addition, except for the last point in the graph, in which 20 mM $MgCl_2$ have been added to a 150-mM NaCl solution to mimic physiological concentrations. As the ionic strength increases, the net ζ-potential value increases, reflecting that indeed positive cations may adsorb on the surface of the polar head of the phospholipid molecule. It is widely accepted that most natural membranes are negatively charged because of the presence of variable quantities of negatively charged phospholipids, yielding surface charges on the order of -0.05 C/m^2 (1). However, in this case, we have to take into account that even though phosphatidylcholine (PC) heads are zwitterionic and thus theoretically globally uncharged at neutral pH, it gives rise to a negative ζ-potential value (-12.0 ± 1.6 mV) in mQ water. This has been interpreted in terms of hydration layers formed around the surface (40) and to the orientation of lipid headgroups (6).

The process of vesicle fusion to flat bilayer is assumed to be electrostatically governed, and it is assumed that surface free energy plays a key role (41). Freshly cleaved mica is negatively charged upon a wide range of ionic strength (40), so that according to Fig. 1 the higher the ionic strength, the higher and the faster will be the adhesion of DMPC liposomes to the mica surface. This process will be especially favored at high ionic strength, where the surface ζ-potential is positive (6.86 $\pm$ 2.3 mV). The probable divalent cation preference for membrane binding may also help to reverse the obtained net ζ-potential value (from negative to positive values). Fig. 2 shows AFM contact mode images of DMPC

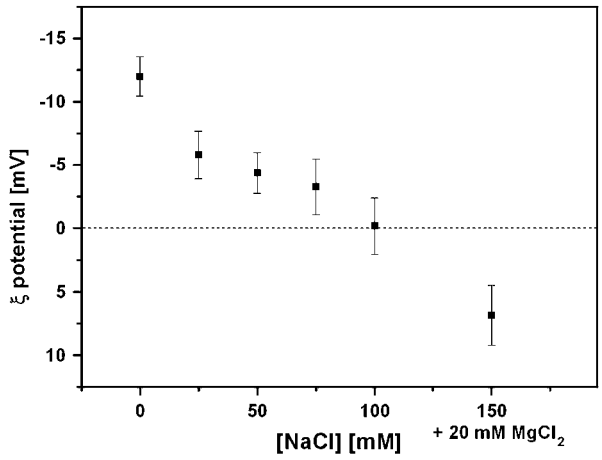

FIGURE 1 ζ-Potential values of the DMPC liposomes versus ionic strength of the measuring solution. Every point in the graph is the average of 15 independent measurements. Error bars represent standard deviation values.

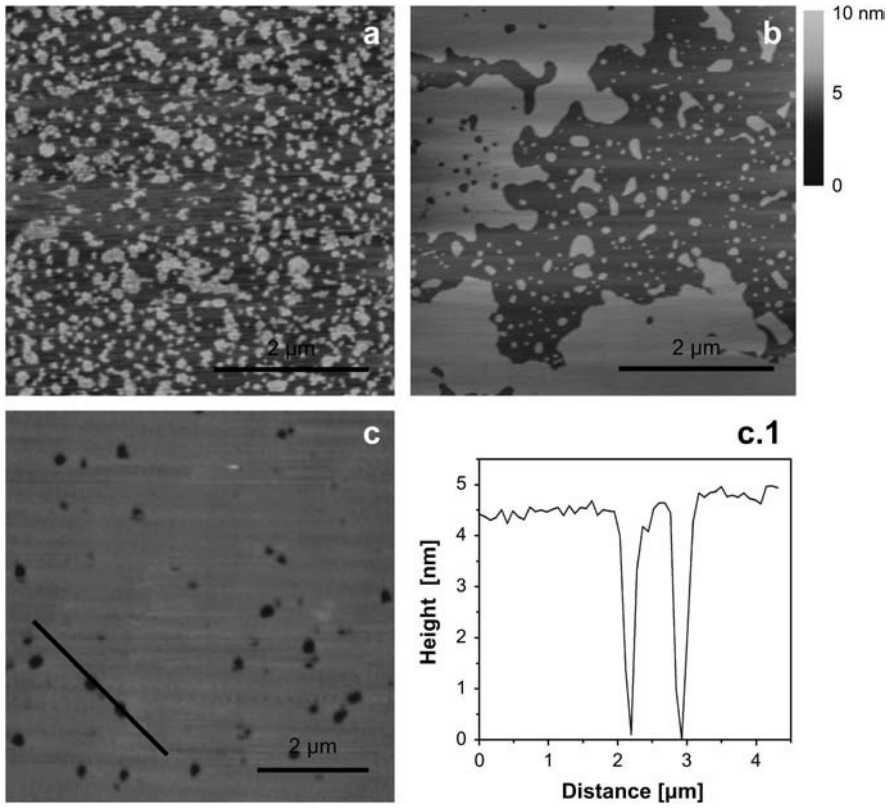

FIGURE 2 AFM contact mode images (5×5 μm^2) of DMPC bilayers in (*a*) distilled water, (*b*) 100 mM NaCl solution, and (*c*) AFM contact mode images (7×7 μm^2) of DMPC bilayers in 150 mM NaCl + 20 mM $MgCl_2$. All solutions were buffered to pH 7.4 with 10 mM Hepes/NaOH. (*c.1*) Cross-section profile of the marked area in *c*. All images were taken after 35 min of liposome deposition.

bilayers as the ionic strength of the surface is increased, showing that the degree of surface coverage is strongly dependent on the amount of ions present in the system. Fig. 2 *a* shows a 5×5-μm^2 contact mode image of DMPC bilayer in distilled water, Fig. 2 *b* shows the image in 50 mM NaCl, and Fig. 2 *c* shows a 7.5×7.5-μm^2 image of DMPC in 150 mM NaCl + 20 mM $MgCl_2$ 10. Fig. 2 *c.1* shows a cross section of the marked area in Fig. 2 *c* in which, thanks to the surface defects, the bilayer height can be measured at ~4.5 nm.

A series of 500-μM DMPC solutions in Millipore water with different ionic strengths (0 mM, 50 mM, 75 mM, and 100 mM NaCl or 150 mM NaCl + 20 mM $MgCl_2$, all with 10 mM Hepes, pH 7.4) were deposited onto a freshly cleaved mica surface and mounted on a Molecular Force Probe1-D liquid cell.

Force curves (Fig. 3) exhibit a breakthrough feature (*black arrows*) in the approaching curve corresponding to the penetration of the bilayer by the tip apex and indicating that the lipid bilayer is not able to withstand the force exerted by the tip. Concerning the retracting curve we observe an adhesion peak, which corresponds to the adhesion between the silicon nitride tip and the surface. The width of the jump (~4.5 nm) corresponds to the height of the bilayer (cross section in Fig. 2 *c.1*). In Fig. 3 *a*, the breakthrough force (also called yield threshold) occurs at ~15 nN. This curve has been taken in a solution of 150 mM NaCl + 20 mM $MgCl_2$. In Fig. 3 *b*, the force plot was taken on a DMPC bilayer in distilled water and the yield threshold is found at ~2.2 nN, which is ~7 fold lower.

Fig. 4 shows the histograms of the yield threshold force values ranging from 2.76 ± 0.11 nN in pure water to 14.93 ± 0.09 nN in buffered high ionic strength solution. Those histograms have been obtained taking only the successful indentation recordings (we call a successful recording the one that presents a breakthrough in the force plot). As we have already clearly seen in Fig. 2, the higher the ionic strength, the higher the degree of coverage of the surface. Thus, the probability of a successful recording is higher as we increase the ionic strength of the solution. In the cases in which the bilayer presents uncovered regions (e.g., Fig. 2, *a* and *b*), when an unsuccessful force plot occurs it means that we are attempting on an ''empty'' area, and we normally observe a typical silicon nitride-bare mica force plot. All histograms here shown belong to the same sample. However, maximum variations of 15–20% have been found between histograms in different experiments (e.g., different sample, different tip).

In Fig. 5, a graph showing the yield threshold force versus the different ionic strengths is shown. Every point in the graph corresponds to the Gaussian center of the Gaussian fit to the data of the histograms shown in Fig. 4. Clearly, the increase in ionic strength gives rise to an increase in the force required to puncture the bilayer. This dependence gives rise to a linear relationship between force and ionic strength (slope ~70 pN/mM). (To obtain this linear fit, the last point in the graph has been supposed as a first approximation to be 210 mM to account for the double charged Mg^{2+} effect.) Here we must point out that all experiments have been

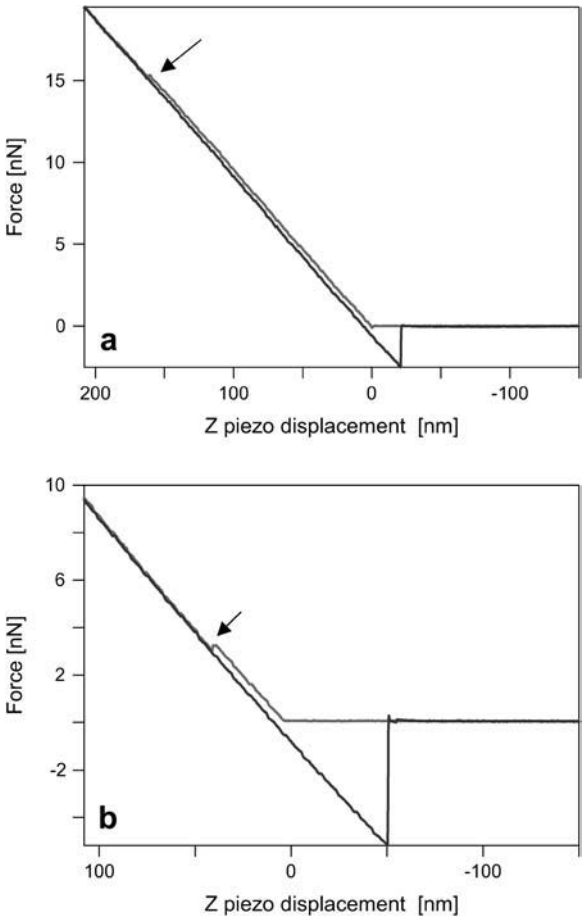

FIGURE 3 Force versus z-piezo displacement plot for a DMPC bilayer in (a) 150 mM NaCl + 20 mM $MgCl_2$ and (b) distilled water. Yield threshold is denoted by black arrows at~15 nN (a) and~2.1 nN (b). The width of the jump, ~4.5 nm, corresponds well with the bilayer height measured using contact mode AFM.

performed at the same indenting velocity (400 nm/s) so that the small effect of velocity on the breakthrough force would not impact the results.

It is important to point out that in a few cases a double jump in the force plots has been observed (Fig. 6). This double jump has been interpreted (42) as a second lipid bilayer that has been formed on the tip. Interestingly, we have only observed double jumps under high ionic strength conditions (~10% of the total force plots under 100 mM NaCl and ~15% of the total force plots under 150 mM NaCl + 20 mM $MgCl_2$ buffered solution); they have never been observed under lower ionic strength concentrations. Due to the slightly negatively charged silicon nitride surface (-0.032 C/m^2 at pH 7.0) (43), bilayer deposition onto the tip may be favored at high ionic strength in a process parallel to that observed for mica. Another experimental issue supporting this fact is that this second jump has never been observed when carboxyl chemically functionalized tips were used, even in the presence of high salt concentration, highlighting again the role of surface free energy upon bilayer

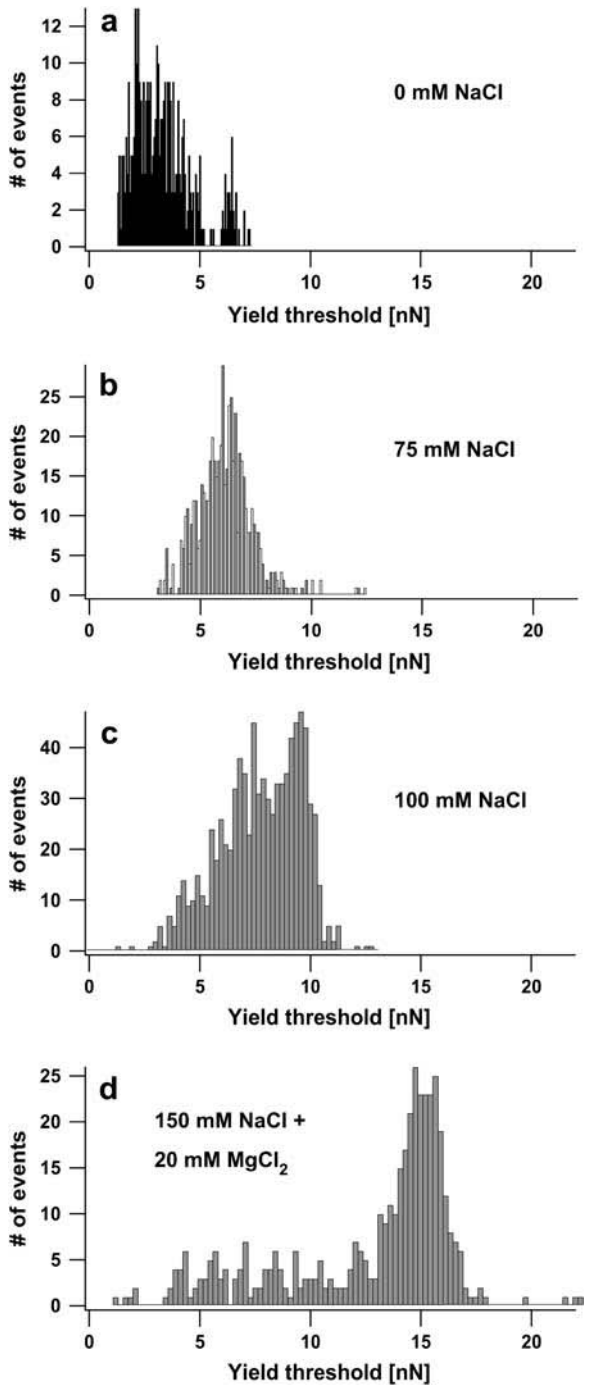

FIGURE 4 Histograms corresponding to the yield threshold force value for DMPC bilayers under different ionic compositions: (a) 0 mM NaCl, $x = 2.76 \pm 0.11$ nN ($N = 396$); (b) 75 mM NaCl, $x = 6.04 \pm 0.04$ nN ($N = 568$); (c) 100 mM NaCl, $x = 7.98 \pm 0.13$ nN ($N = 872$); and (d) 150 mM NaCl + 20 mM $MgCl_2$, $x = 14.93 \pm 0.09$ nN ($N = 427$). All results correspond to a Gaussian fitting of the data shown in the histogram. Results are presented as the Gaussian center $x \pm 2s/\sqrt{N}$.

deposition. These results are in agreement with those observed by Pera et al. (42) and Franz et al. (29), which correlated the presence of the second jump with salt concentration. The force plot recordings where two jumps have been observed

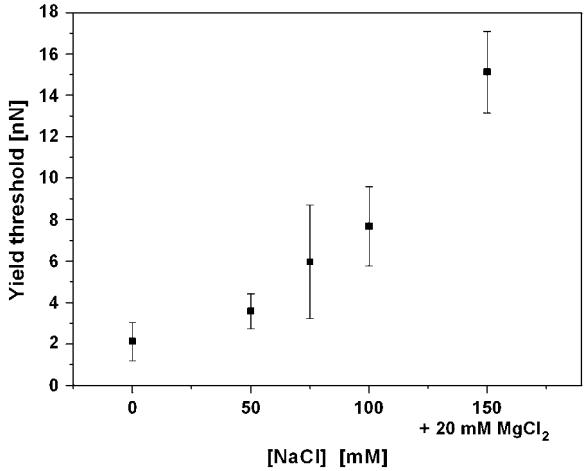

FIGURE 5 Yield threshold values versus ionic NaCl concentration for all the obtained force plots on DMPC bilayers shown in Fig. 4. Each point in the graph corresponds to the central value of the Gaussian fit to the histograms shown in Fig. 4. Error bars represent standard deviations within the same experiment.

have not been taken into account for data statistics (Figs. 4 and 5).

To understand the nature of the sudden breakthrough (jump in the force plot), we have to take into account the interactions that arise between phospholipid molecules. Apart from hydrophobic interactions between neighboring tails, the PC head contains groups that are negatively charged (the oxygen of the phosphate group) and positively charged (the quaternary amine in the choline moiety). Two major classes of short-distance interactions occur between the PC headgroups. One is the formation of water cross-bridges between negatively charged groups in which a water molecule is simultaneously hydrogen-bonded to two PC molecules. Each DMPC molecule is bridged on average to 4.5

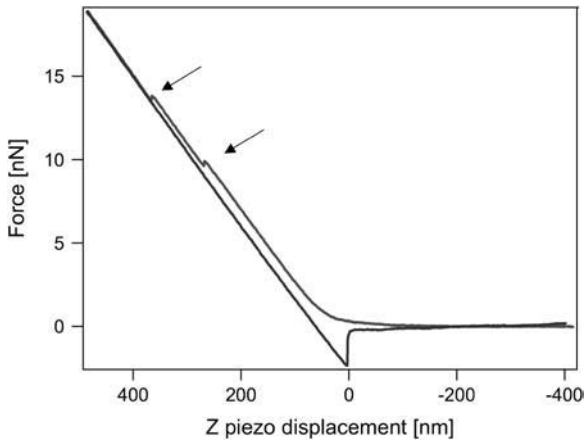

FIGURE 6 Force plot on a DMPC lipid bilayer under high ionic strength conditions (150 mM NaCl + 20 mM $MgCl_2$) where a second jump in the force plot occurs, probably due to a second lipid bilayer deposited on the silicon nitride AFM tip apex. This second bilayer may be stabilized by the presence of salt.

water molecules (44). The second class involves charge associations (charge pairs) formed when the oppositely charged groups are located within 4 Å of one other. Recent MD simulations (45) found that 98% of DMPC molecules are linked via water bridges and/or choline-phosphate and/or choline-carbonyl charge pairs to form long-lived clusters giving rise to a huge network of interactions. In particular, 90% of all PC molecules are linked to each other through such charge pairs. This result suggests that headgroup-headgroup interactions greatly contribute to the stability of the membrane and that electrostatic interactions play a key role in membrane stability even though PC is a zwitterionic species at neutral pH. This electrostatic nature is in good agreement with the sudden jump in the indentation curve. In earlier works, we proved that ionic single crystals break layer by layer in discrete jumps because of electrostatic repulsions between ions in the lattice as the AFM penetrates the substrate (19). Interestingly, the force at which an ionic single crystal breaks (~60 nN for a KBr single crystal) is of the same order of magnitude as that observed for a lipid bilayer. This fact alone may explain the shape of the breakthrough (brittle material), but cannot explain the increase of the force value at which this jump occurs in the presence of cations in the surrounding medium.

As we have observed, the ζ-potential value increases as the ionic strength is increased. To deal with the increase in surface charge upon cation binding we can calculate the surface charge related to the ζ-potential value obtained for each different ionic strength (Fig. 1) through the simplified Grahame equation for low potentials (46):

$$\sigma = \varepsilon\varepsilon_0\kappa\psi_0, \tag{1}$$

where σ stands for the surface charge, κ stands for the reciprocal of the Debye length, and ψ_0 stands for the surface potential. The surface charge values are -2.12×10^{-3} C/m^2 at 25 mM ionic strength, -1.30×10^{-4} C/m^2 at 100 mM ionic strength, and 6.89×10^{-3} C/m^2 at 150 mM NaCl + 20 $MgCl_2$. Those values are in agreement with those found in Marra and Israelachvili (47). However, they are far too low to explain the high Na^+ and Mg^{2+} coordination numbers found upon MD simulations. The surface charge calculated through the Gouy-Chapman theory assumes that the interface between the membrane and aqueous solution is planar with zero width and that the charge on the membrane is homogeneously distributed on the membrane surface in a continuous way. This assumption has proved in MD simulations to be rather dramatic in the case of a membrane/aqueous solution interface. Even in this case, simulations predict a surface potential similar to the obtained values through ζ-potential experimental measurements (Gouy-Chapman model) for distances >10 Å from the bilayer surface (8). Therefore, the Gouy-Chapman model theory describes qualitatively well the membrane/solution interface for distances >1 nm away from the ''real'' membrane surface. The huge discrepancy between the potential values obtained

through MD simulatons upon ion binding and through ζ-potential measurements may lie roughly within this nanometer interface. According to DLVO theory, using the above surface charge values, we can calculate the electrostatic interaction arising between the AFM tip and the bilayer as the tip approaches the bilayer by combining electrostatic and van der Waals forces:

$$F_{\mathrm{DLVO}} = F_{\mathrm{el}(z)} + F_{\mathrm{VdW}} = \frac{4\pi\sigma_{\mathrm{DMPC}}\sigma_{\mathrm{tip}}R_{\mathrm{tip}}\lambda}{\varepsilon_0\varepsilon} e^{-z\lambda} - \frac{H_{\mathrm{a}}R_{\mathrm{tip}}}{6z^2}, \quad (2)$$

where σ_{DMPC} and σ_{tip} are the surface charges for the DMPC bilayer and the tip, respectively, R_{tip} is the radius of the tip, and λ stands for the Debye length. H_{a} is the Hamaker constant and z is the distance between the sample and the tip. Considering $H_{\mathrm{a}} = 10^{-21}$ J (47), $\sigma_{\mathrm{tip}} = -0.032$ C/m^2 at pH 7.0, and a mean area/molecule of 0.5 nm^2 (48), and taking the obtained values for the surface charge at different ionic strengths, we can obtain the interaction force between the bilayer and the tip. Table 1 shows the results corresponding to the surface charges and the interaction forces at different ionic strengths using bare silicon nitride tips.

Silicon nitride tips were used to perform force spectroscopy experiments. At neutral pH, those tips are known to be slightly negatively charged, although there is a great variability between individual tips. As can be seen from Fig. 3, no important repulsion or attraction (jump to contact) can be observed upon force plots performed with the low negatively charged Si_3N_4 tips. Therefore, it seems that the breakthrough force cannot be (totally) explained in terms of electrostatic interaction between tip and sample. To have chemically controlled tips (negatively charged at neutral pH), and to address the question of to what extent electrostatic interactions can play a role in the membrane breakthrough, we have functionalized gold-coated AFM tips with 16-mercaptohexadecanoic acid (p$K_{\mathrm{a}} = 4.7$), surface potential ~ -140 mV (23), and we have performed force plots in the sample in the absence of salt (ζ-potential $= -12.0 \pm 1.6$ mV, first experimental point in Fig. 1) and under high ionic strength (ζ-potential $= 6.86 \pm 2.3$ mV, last experimental point in Fig. 1). A slight repulsion is observed when both tip and surface are negatively charged (Fig. 7 *a*) and a small jump to contact ($\sim$220 pN) is seen when the tip is negatively charged and the surface is positively charged (Fig. 7 *b*). The repulsion force is higher when the force plots are performed at basic pH values (pH 9–12, more negatively charged surface) and the jump to contact becomes greater at lower pH values (data not shown). The obtained results at pH 7.4 totally agree with the results predicted upon DLVO theory calculations for the interaction of a carboxyl-terminated tip and the bilayer surface at different ionic strengths (Table 1). Briefly, in distilled water, the surface is negatively charged, and so is the tip. Therefore, the interaction force will be repulsive and it will be lower than 260 pN. In high ionic strength solution, the surface is positively charged, so the jump to contact is also predicted according to DLVO calculations. Likewise, here we have to point out the ability

TABLE 1 DLVO parameters for the interaction of the AFM tip and the studied surface when the tip is bare silicon nitride or carboxyl-terminated

[NaCl] (M)	λ (nm)	σ_{tip} (C/m^2)	$\sigma_{\mathrm{DMPC}} \times 10^3$ (C/m^2)	DLVO force (nN)
Silicon nitride tip				
0.025	1.92	−0.03	−2.12	0.00760
0.05	1.358	−0.05	−2.25	0.015
0.075	1.108	−0.06	−2.07	0.004
0.1	0.96	−0.06	−1.31	Attraction
0.15 + 0.02 $MgCl_2$	0.662	−0.09	6.89	Attraction
Carboxyl-terminated tip				
0.025	1.92	−0.15	−2.12	0.26
0.05	1.358	−0.21	−2.25	0.44
0.075	1.108	−0.25	−2.07	0.51
0.1	0.96	−0.29	−0.131	0.009
0.15 + 0.02 $MgCl_2$	0.662	−0.51	6.89	Attraction

The terms λ, σ_{tip}, and σ_{DMPC} stand for the Debye length, the tip surface charge, and the bilayer surface charge, respectively, for both tips.

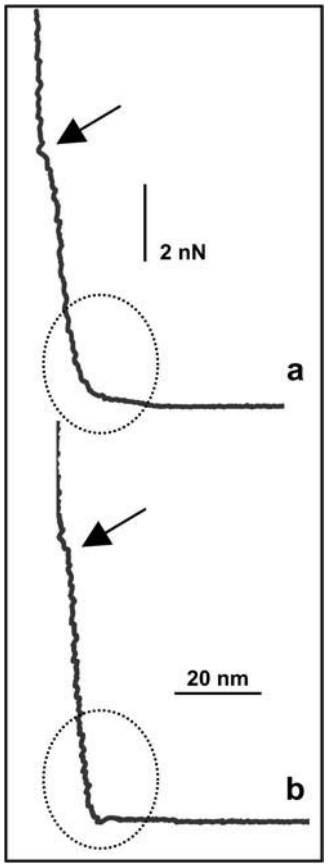

FIGURE 7 Force plots obtained as a 16-mercaptohexadecanoic acid approaches a DMPC bilayer under (*a*) distilled water, 10 mM Hepes, pH 7.4, negative surface charge; and (*b*) a 150 mM NaCl + 20 mM $MgCl_2$ solution, 10 mM Hepes, pH 7.4, positive surface charge. Yield threshold is indicated by an arrow.

of chemically modified tips to sense surface charges, even when they are of a few mC/m^2. In any case, the repulsive forces are <1 nN and thus in both curves the yield threshold point (*arrow*) clearly occurs at a much higher force than the electrostatic interaction force regime here presented.

Hydration and steric forces have been described as responsible for short-distance repulsion between two opposing lipid bilayers. Indeed, it is the force needed to remove the water molecules adsorbed on amphiphilic groups as both surfaces come into contact (46). It has been shown that the role of water is extremely crucial to membrane stability. It is therefore quite straightforward to think that hydration force may play a role in membrane mechanical stability. Therefore, if water was replaced with, e.g., ethanol, the overall network created by the H-bonds would be partially disrupted and therefore one might expect that the yield threshold would be much lower (that is to say, lateral interactions between phospholipid molecules in the membrane would be reduced so that it would be easier for the tip to penetrate the membrane). Indeed, it has been reported that short-chain alkanol, such as ethanol, displaces water from the network with an overall effect of weakening lipid-lipid interactions by increasing headgroup spacing (higher area per lipid) (49). To address the question of whether this decrease in lateral interactions has any effect on the nanomechanics of the system we have formed a DMPC bilayer under water and, once formed, replaced water with an EtOH/water solution (50:50%, $x_{\text{ethanol}} = 0.72$). Immediately after the solution was added, a clear decrease in the rupture force was observed down to ~0.5 nN, as shown in Fig. 8. Interestingly, no membrane disruption was observed, since in 100% of the cases a jump (break) in the force plot was observed (if the membrane had been disrupted, the retracting curve of the force plot would have shown not a clear adhesion peak, indicating the sudden snap-off from the surface, but a continuous, nonreproducible feature that indicates that material is being pulled off the surface. In this case, when membrane is disrupted (for concentrations higher than 75:25%, ethanol/water), no jump in the extending force plot is observed since membrane is not packed enough). These results are in agreement with AFM images, in which membrane dissolution was not observed upon ethanol addition, and the only observed feature was the growing of small holes in the system, suggesting a less compact structure. Similar results have been obtained when the bilayer has been formed under high ionic strength. In this case, the yield threshold values both before and after ethanol addition were shifted to higher values on account of the cations present in the bilayer. It seems clear, then, that water plays a key role in membrane structure and that this fact has a direct effect on membrane mechanical deformation.

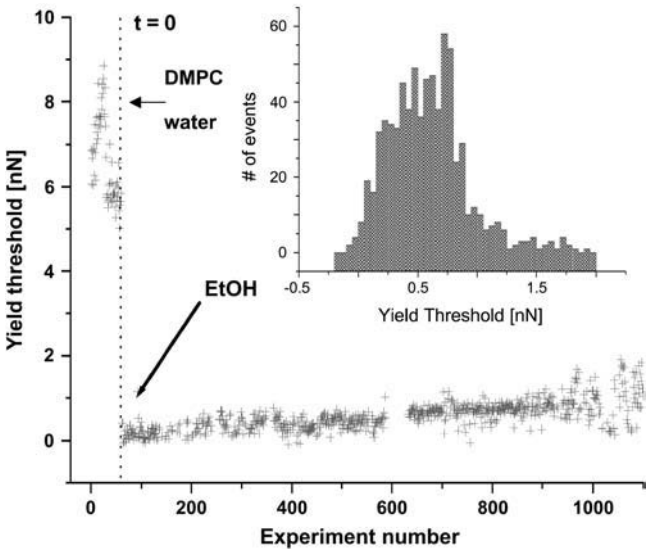

FIGURE 8 Evolution of the force at which the yield threshold occurs after the addition of a 50:50% ethanol/water solution. After addition of ethanol the yield threshold force value occurs at $x = 0.533 \pm 0.03$ nN ($N = 734$) (Gaussian fit to the histogram).

Hydration force has been reported (27) to extend to ~5 nN and cannot alone explain the force-distance curves acquired with AFM until the breakthrough point. This hydration force is short-ranged and follows the expression

$$F_{\text{hydration}} = F_0 e^{-(z/\lambda)}, \tag{3}$$

where F_0 is the preexponential factor, z is the separation between the surfaces, and λ is the hydration decay length. Typically, $F_0 = \sim 0.15$–2 nN and $\lambda = 0.2$–0.35 nm for measurements performed with a surface force apparatus (46) and 2–5 greater for measurements performed by AFM between lipid bilayers and alkanethiol-functionalized probes(27). Instead, a mechanical contribution accounting for the elastic deformation of the bilayer was needed to fully account for the force-distance shape of the curve until the plastic regime was achieved (27).

Molecular dynamics simulations have recently demonstrated (7,9,35) that the presence of cations (namely, Na^+ and Ca^{2+}) in the phospholipid network would change drastically the structural and dynamical properties of the PC membranes. On average, every Na^+ cation binds to three carbonyl oxygens and to one to two water oxygens. Due to their threefold increased size as compared to single lipids, these complexes are less mobile. As a consequence, a decrease in the average area per lipid from 0.655 nm^2 to 0.606 nm^2 (>8%) is observed for POPC, giving rise to a more compact overall structure. Indeed, the difference in the area per group is also reflected by the ordering of the lipid hydrocarbon tails (7,9). A similar case applied to Ca^{2+}, each Ca^{2+} cation binding to 4.2 PC heads on average. The same MD simulations revealed that despite those significant changes, the profile of the total electric potential across the bilayer for distances >10–18 Å from the center of the bilayer is only slightly changed due to the close distribution of Cl^- counterions giving rise to a strong capacitor, and especially to the fact that water molecules reorient their dipoles near the

membrane surface (distances <10 Å). It is well known that for distances less than this, water molecules do not exhibit bulk-like properties (8). Overall, the total electric potential a nanometer away from the surface does not change as much as one would predict at first sight, and these results are in very good accordance with the (low) values obtained upon ζ-potential measurements, even when they demonstrated the same tendency to increase in value as the ionic strength is increased. Therefore, and according to those molecular dynamics simulations, the higher-order structure promoted by ions on the bilayer that give rise to a the reduction in average area per lipid (higher compactness) and to a more rigid structure (lower diffusion coefficient) may be the cause for the higher membrane stability experimentally observed through the nanomechanical response of the system obtained by force spectroscopy measurements. It seems then that rather than drastically increasing the electrostatic potential across the membrane (z direction) the introduction of ions in the membrane gives rise to a much higher lateral interaction within neighboring headgroups, with the overall result of a higher packing and compactness of the whole network composing the membrane. This increase in the lateral forces (closer distance between individual molecules) is probably the last responsible for membrane higher resistance upon breaking. This fact is in very good agreement with earlier results obtained for halide single crystal nanoindentation (19), where we demonstrated both experimentally and theoretically that the yield threshold force value was dependent on the anion-cation distance in the lattice (a lower ion distance gave rise to a higher yield threshold force value, e.g., for NaCl compared to a compound, such as KBr, with higher ion-cation distance) in a single-crystal study of a series of alkali halides. To elucidate the role that those reported lateral interactions within the phospholipid network play upon membrane deformation we have applied a simple model that we proposed elsewhere (19), which takes into account the lateral interactions while the surface is being deformed by an AFM tip. Those lateral interactions are modeled by the dynamics of the deforming surface as n coupled springs. According to this model, the dependence of the surface counterforce opposing the AFM tip penetration follows the expression

$$F(\delta) = k\delta\left(1 - d_s/\sqrt{\left(\delta^2 + d_s^2\right)}\right), \tag{4}$$

where k and d_s stand for an effective spring constant equal to the Debye wavevector and the length at zero elongation, respectively. Fig. 9 shows the indentation plot of a DMPC bilayer measured in aqueous solution, 25 mM NaCl, pH 7.4, until the jump (onset of the plastic deformation) occurs. The elastic spring model (4) has been fitted to the experimental data after the first ~100 pN (electrostatic interaction) up to the yield threshold. The fit to the model is shown in Fig. 9 with a continuous shaded line. As is clear from the graph, the fit describes quite well the elastic deformation region of the indentation plot. This fit gives rise to a k value of 17.1 N/m

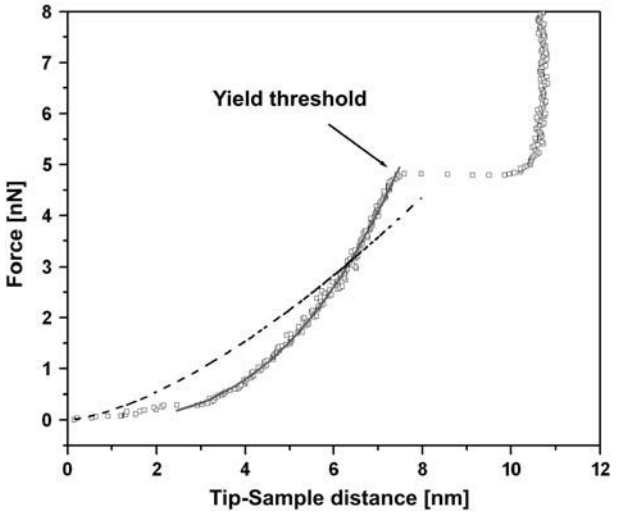

FIGURE 9 Force-distance curve corresponding to the indentation of a DMPC bilayer under 25 mM NaCl, pH 7.4. The elastic region (up to the yield threshold point) has been fitted (*a*) to the spring model (*continuous shaded line*) and (*b*) to the Hertz model, taking $R = 31$ nm (*dashed line*).

and a d_s value of 26.1 nm. The k value indicates the stiffness of the surface upon deformation, whereas the d_s value indicates the whole perturbed length before breaking. Interestingly, this d_s value is much higher than those found for alkali halide single crystals ($d_s = 0.9 \pm 0.3$ nm for NaCl) indicating that deformation is a cooperative process in which many molecules are involved in the membrane deformation before breaking (the deformed area being much greater than the contact radius itself). In the case of a solid alkali halide single crystal this plastic failure occurs because the charge repulsion within the lattice is so strong that the surface is not able to deform anymore, giving rise to a brittle failure in a fast layer-by-layer plastic deformation process. Besides, the ratio between the obtained k and d values gives rise to 337 MPa, which is a value similar to the reported reduced Young modulus for distearoylphosphatidylethanolamine (170 MPa). This ratio yields similar values to Young modulus values for ionic systems, but fails for nonionic (covalent) systems, suggesting that lipid bilayer deformation can be partially governed by electrostatic interactions. The simple spring model was used to describe elastic deformation of surfaces in the nanometer range after realizing that the Hertz model did not succeed in describing elastic deformation at this scale, which is not surprising since the Hertz model is a macroscopic model and its boundary conditions are not fulfilled upon indentation with an AFM tip and also since we must take into account that the substrate is relatively hard as compared to the organic layer (50). For a paraboloid indenter, the Hertz equation yields

$$F = 4/3\, E * R^{1/2}\delta^{3/2}, \tag{5}$$

where E^* stands for the reduced Young modulus. That the elastic regime of lipid bilayers cannot be described by

the Hertz equation has been recently stressed (30). A fit of the experimental data to the Hertz model is also included in Fig. 9, taking $R = 31$ nm (individually measured by imaging a silicon calibration grid, Micromasch, Ultrasharp, TGG01, silicon oxide), and letting E^* be the free variable (*dashed line*). As can be easily seen, the Hertz model does not reproduce the experimental data, whereas the spring model can adjust the experimental data. Besides, an exponential-growth equation accounting for hydration forces (3) has been also applied, but the hydration decay length (λ) yields an unrealistic value of 2.8 nm. If a decay length of 0.35 nm is fixed, the equation does not reproduce the experimental data at all. Therefore, a mechanical deformation component of the bilayer seems to be the factor responsible for most of the repulsive regime between the AFM tip and the lipid bilayer, at least after the first nanometer separation. Similar results were reported for distearoylphosphatidylethanolamine bilayers (27).

Kinetics

The incorporation of ions into the PC headgroup can be finally proved to be a fully reversible process with relatively fast kinetics in the timescale of the experiment: a compact lipid bilayer was formed in the physiological solution (150 mM NaCl + 20 mM $MgCl_2$), we measured the yield threshold value, and, once done, we replaced the solution with distilled water. The yield threshold decreased to a value of $\sim$6.2 $\pm$ 0.12 nN, increasing again to $\sim$15.9 $\pm$ 0.15 nN when water was replaced with the former solution (Fig. 10). The waiting time from changing the solution and measuring was $\sim$10 min in each case. In the same line, we studied the direct evolution of the yield threshold with time while changing the measuring solution by recording >3000 consecutive force plots in the same spot of the surface over more than 1 h (Fig. 11). Until about experiment 1200, the measuring solution was water. Then, water was removed and replaced with the former high ionic strength physiological solution. The yield threshold varied from $\sim$3 nN to $\sim$15 nN in $\sim$15 min, and even though there is some scattering in the data after experiment 1750 (maybe on account of not totally homogeneous distribution of ions), a more or less stable value plateau was reached. Thus, taking into account the region between the two plateaus we can roughly assess that the kinetics of the system has a rate constant of $\sim$0.7 nN/min. This fact indicates that the process of binding cations is not an instant process. In any case, the kinetics of the process is experimentally measurable within the AFM timescale.

So far we have proved that the ionic strength gives rise to a huge increase in the force needed by the AFM to penetrate the membrane for a DMPC bilayer. The next step is to assess whether this process takes place with other PC bilayers and also with bilayers composed of phospholipids with other zwitterionic heads.

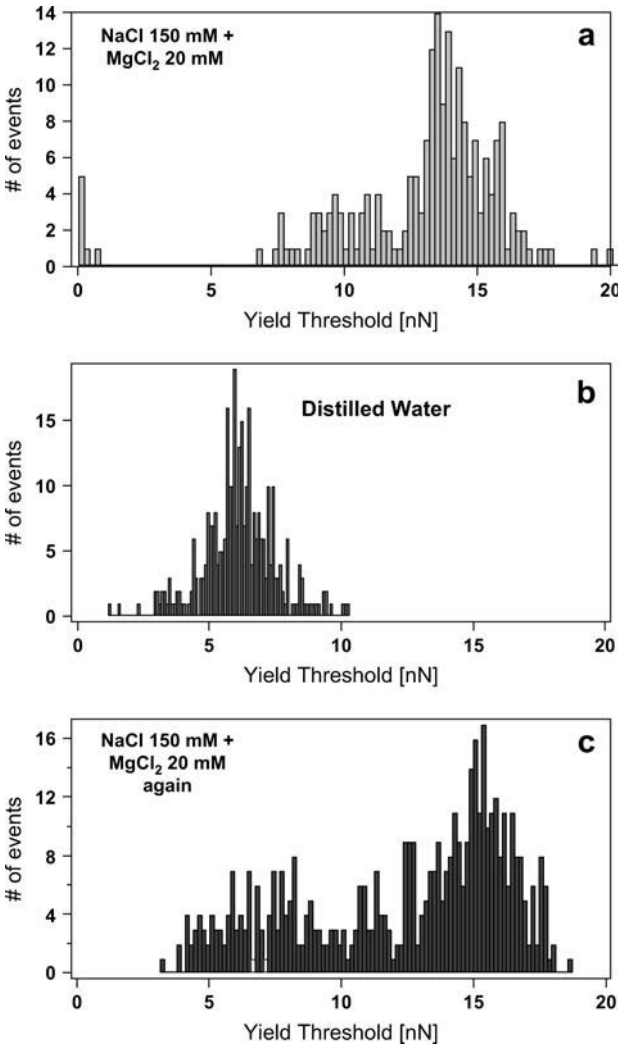

FIGURE 10 Histograms of the yield threshold force value for DMPC bilayers under different ionic strength values: (*a*) 150 mM NaCl + 20 mM $MgCl_2$, $x = 14.12 \pm 0.16$ nN ($N = 350$); (*b*) 0 mM NaCl, $x = 6.2 \pm 0.12$ nN ($N = 328$); and (*c*) 150 mM NaCl + 20 mM $MgCl_2$, $x = 15.9 \pm 0.15$ nN ($N = 483$). The measured bilayer is the same in all three cases: Once the bilayer is formed and measured at a high ionic strength, the solution is replaced with water, measured again, and then water is replaced with the former solution.

PC bilayers: effect of ion-binding and phospholipid chemical structure

Dealing with PC bilayers, we have performed the same experiment with DLPC and DPPC, which only differ from DMPC in the number of $-CH_2$ groups in the fatty acid chain. Fig. 12 shows the histograms corresponding to the yield threshold value for a DLPC membrane measured in water (Fig. 12 *a*) and in high ionic strength physiological solution (Fig. 12 *b*). The yield threshold value shifts from 3.78 $\pm$ 0.04 nN in the case of water to 6.12 $\pm$ 0.08 nN for high ionic strength physiological solution. Data for DMPC measured in water (Fig. 12 *c*) and in high ionic strength physiological solution (Fig. 12 *d*) are also included for the sake of

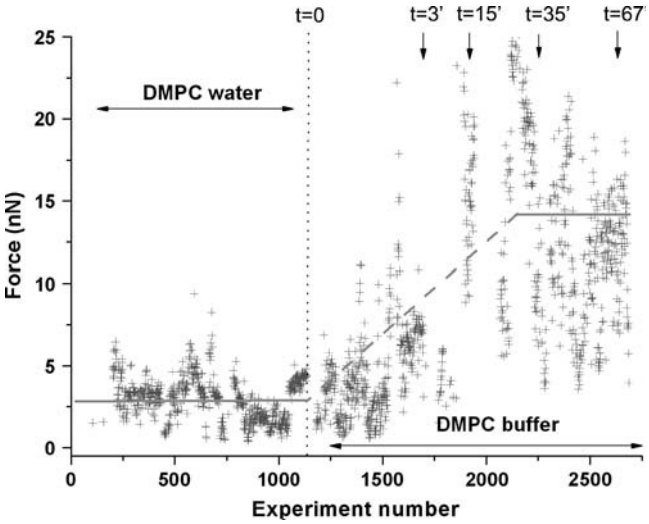

FIGURE 11 Evolution of the yield threshold force value with time in the same spot of the surface (ignoring drift) along an experiment in which water was replaced with high ionic strength solution (*dotted line*). Theh time was set to zero as high ionic strength solution was added. After ~15 min a more or less stable plateau is reached. The orange line is meant to guide the eye.

comparison. Similarly, Fig. 12, *e* and *f*, shows the histogram for DPPC measured in water and in high ionic strength physiological solution, respectively. Again in this case the effect of ionic strength (I) is clear, since the breakthrough force is 7.02 ± 0.06 nN when measured in water solution and 20.31 ± 0.29 nN when measured at high ionic strength. Fig. 12 *h* shows the change in ζ-potential value as the ionic strength of the medium is increased from 0 mM (distilled water) to 100 mM NaCl for four different PC liposomes, namely DLPC, DMPC, DPPC, and DOPC. In all cases, the higher the ionic strength, the higher (less negative) the ζ-potential value, meaning that in all cases there is adsorption of monovalent cations in the membrane, which can be again easily correlated with the nanomechanics of the systems (Fig. 12, *a–f*). In light of these results, in which phospholipids with the same headgroup (PC) and different chain length have been studied, the effect of the chemical structure of the phospholipid tail on the nanomechanical response of the bilayer can also be addressed. The comparison of the yield threshold force values obtained for the previous PC bilayers, i.e., DLPC (12:0), DMPC (14:0), and DPPC (16:0), where numbers in parentheses represent number of carbon atoms in the fatty acid chain per number of insaturations (Fig. 12, *a–f*), are summarized in Fig. 12 *i*, where the relationship between the yield threshold force value and the number of carbon atoms present in the fatty acid of the phospholipid molecule composing the bilayer is shown. Dark squares stand for the measurements performed under high ionic strengths (Fig. 12, *b*, *d*, and *f*) and white squares stand for the measurements performed in distilled water (Fig. 12, *a*, *c*, and *e*). According to Fig. 12 *i*, the effect of ionic strength on the nanomechanics of the system is evident for the three PC phospholipids studied. However, this effect is especially outstanding in the case of DMPC and DPPC (yielding a yield threshold force value increment, ΔF_y, between the measurements obtained under high ionic strength and those obtained under distilled water of ~11 nN in the case of DMPC and ~14 nN in the case of DPPC). This yield force value increment is smaller in the case of DLPC ($\Delta F_y = \sim 3$ nN). This result could be interpreted in terms of the phase in which the different phospholipids are present. Although DLPC ($T_M = -1°C$) is in the liquid phase at 20°C, DMPC ($T_M = 24°C$) and DPPC ($T_M = 42°C$) are both in the gel phase at this temperature. Therefore, these results suggest that although ion binding has influence on both the gel phase and the liquid phase, it is in the gel phase that this effect is more enhanced. We have recently addressed the effect of temperature on the yield threshold value of lipid bilayers in a systematic study that corroborates these results (S. Garcia-Manyes, G. Oncins, and F. Sanz, unpublished). When comparing the nanomechanical response of the bilayer for the two phospholipids present in the gel phase (DMPC and DPPC) we realize that the longer the tail, the harder it is to puncture the membrane, yielding an increase of ~5 nN for every two extra $-CH_2$ groups present in the hydrophobic tail in the case of measurements performed under high ionic strength and an increase of ~4 nN in the case of measurements performed in distilled water. In this case, where phospholipids are in the same (gel) phase, these differences become a direct measurement of van der Waals interactions between phospholipid neighboring tails. Those results experimentally demonstrate that the length of the hydrophobic chains of the phospholipid molecules indeed have an influence on the nanomechanics of the system. A systematic study concerning the individual effect of the hydrophilic headgroup and the hydrophobic tail for different phospholipids, both charged and zwitterionic, all in the same phase, is an ongoing experiment in our laboratory. Finally, the role of the insaturations in the fatty acid has also been taken into account. We have studied the mechanical response of DOPC (18:1), in which, although the 18 carbon atoms in the chain may predict a higher yield threshold value than DPPC, the insaturation in the chain gives rise to a lower overall packing of the molecule (~30° tilting), clearly yielding a lower resistance to rupture than expected (Fig. 12 *g*), although it is found in the liquid-like phase. The influence of the insaturation degree and also of the stereochemistry of the insaturation (whether this is in the *cis* or *trans* conformation) will also be interesting for future research in this area.

POPE bilayer

To check whether the effect of ion-binding on the mechanical response of the membrane found in PC bilayers is also observed in other zwitterionic phospholipid headgroups, such as PE, we have measured the yield threshold values with two different salt concentrations for a POPE bilayer.

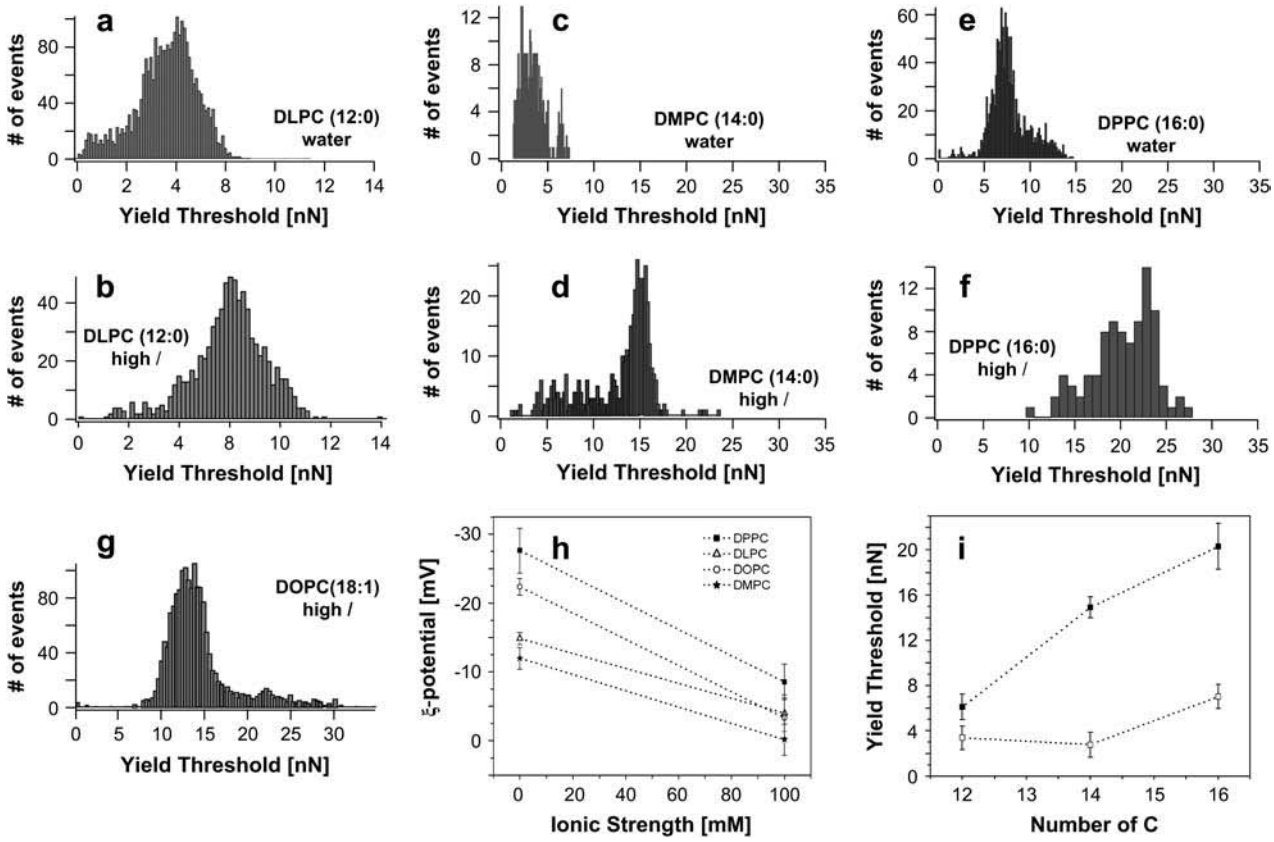

FIGURE 12 (*a* and *b*) Histograms of the yield threshold value for DLPC in water and 150 mM NaCl + 20 mM $MgCl_2$, respectively, where (*a*) $x = 3.78 \pm 0.04$ nN ($N = 2656$) and (*b*) $x = 6.12 \pm 0.08$ nN ($N = 794$). (*c* and *d*) Histograms of the yield threshold value for DMPC in water and 150 mM NaCl + 20 mM $MgCl_2$, respectively, where (*c*) $x = 2.76 \pm 0.11$ nN ($N = 396$) and (*d*) $x = 14.93 \pm 0.09$ nN ($N = 427$). (*e* and *f*) Histograms of the yield threshold value for DPPC in water and 150 mM NaCl + 20 mM $MgCl_2$, respectively, where (*e*) $x = 7.02 \pm 0.06$ nN ($N = 1272$) and (*f*) $x = 20.31 \pm 0.29$ nN ($N = 785$). (*g*) Histogram of the yield threshold force value for DOPC (18:1), where $x = 14.4 \pm 0.10$ nN ($N = 1691$). All results correspond to a Gaussian fitting of the data shown in the histogram. Results are presented as the Gaussian center $x \pm 2s/\sqrt{N}$. (*h*) ζ-Potential values of the PC liposomes as the ionic strength increases. Every point in the graph is the average of 15 independent measurements. Error bars stand for standard deviation value within the measurement. Lines are a guide to the eye. (*i*) Dependence of the yield threshold value for the studied saturated PC as a function of the carbon atoms present in the fatty acid chain. Black squares represent measurements performed under high ionic strength conditions and white squares represent measurements performed in distilled water. Error bars are standard deviations of the measurement. Lines are a guide to the eye.

The same tendency observed with PC is observed with PE despite the different chemical structure of the head. At 50 mM NaCl the yield threshold takes place at 1.63 ± 0.03 nN and increases to 3.43 ± 0.04 nN when measured in a 100 mM NaCl solution. The low yield threshold values compared to those observed for PC phospholipids can be explained in terms of the chemical difference of the headgroup, the chain unsaturation, the phase in which POPE is found at 20°C, or a mixing of all three variables. Further work that will help to shed light on the role of every variable (headgroup effect, chain effect, and temperature effect) in the nanomechanics of lipid bilayers is an ongoing experiment in our laboratory. In any case, the role of ion-binding on PE bilayers seems to follow the same tendency observed for PC bilayers. Since cations seem to bind through the oxygen carbonyl of the phosphate, the observed tendency is then not surprising, and especially if we take into account that MD simulations have shown similar results for phospholipid heads other than PC, such as phosphatidylserine (51), and also for a mixture of phospholipids (8).

Natural *E. coli* bilayer

After having studied the effect of ion binding on model lipid bilayers, the final issue is to check it on a natural lipid bilayer. To this end, we have performed the same experiment on an *E. coli* polar lipid extract (nominally 67% phosphatidylethanolamine, 23.2% phosphatidylglycerol, and 9.8% cardiolipin). In principle, and according to the fact that we have separately proved that both PC and PE membranes are punctured at a higher force as the ionic strength increases, the same result should be expected for this natural membrane extract. Fig. 13, *a–d*, shows the histograms corresponding to the yield threshold values found for *E. coli* membrane, where the same trend is observed. Fig. 13 *e* shows a topographic image of the *E. coli* membrane, and in Fig. 13 *f* the yield

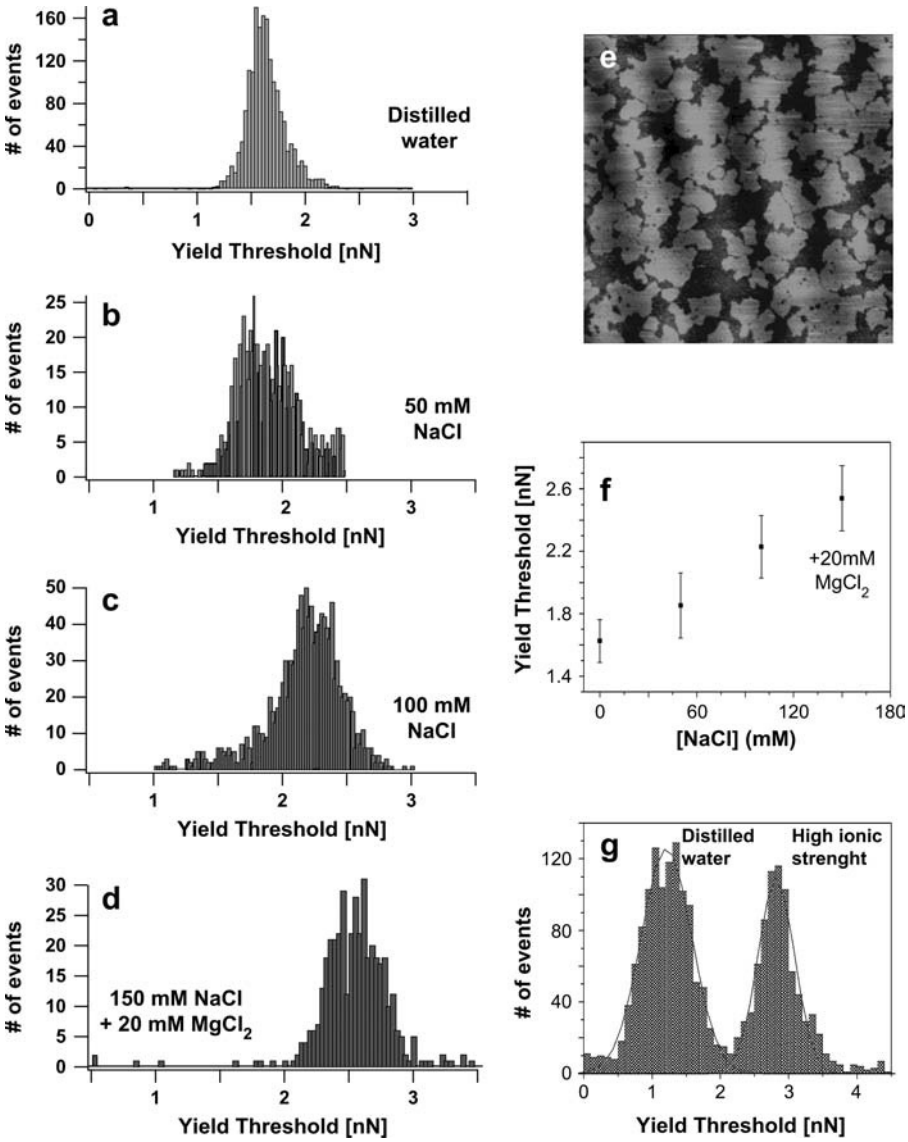

FIGURE 13 (*a–d*) Histograms of the yield threshold force value for *E. coli* bilayers under different ionic compositions: (*a*) 0 mM NaCl, $x = 1.60 \pm 0.14$ nN ($N = 1815$); (*b*) 50 mM NaCl, $x = 1.854 \pm 0.206$ nN ($N = 792$); (*c*) 100 mM NaCl, $x = 2.23 \pm 0.201$ nN ($N = 1252$); and (*d*) 150 mM NaCl + 20 mM $MgCl_2$, $x = 2.54 \pm 0.21$ nN ($N = 591$). All results correspond to a Gaussian fitting of the histograms. (*e*) Contact mode image (5×5 μm^2) of an *E. coli* bilayer deposited on mica. (*f*) Yield threshold values versus ionic strength for the data obtained in histograms *a–d*. Every point stands for the center of the Gaussian fit to the data of the above histograms, whereas error bars represent standard deviations. (*g*) Histograms corresponding to the force plots acquired in distilled water and high ionic strength solution.

threshold force versus ionic strength has been plotted, similar to Fig. 5 for the model membrane. Interestingly, the slope of the plot is ~6 pN/mM, a much lower value than that obtained for the model membrane. Similar results have been obtained for a natural lecithin plant membrane (S. Garcia-Manyes, G. Oncins, and F. Sanz, unpublished). This lower contribution of the added ions on the overall nanomechanical behavior of the system could be interpreted in terms of the complexity of the chemical composition of the system (different phospholipids) that would give rise to a lower packing of the system. However, although this effect is not as outstanding as it was for DMPC, the trend is clearly seen if we compare the histograms for distilled water ($x = 1.60 \pm 0.14$ nN) with those obtained with high ionic strength ($x = 2.54 \pm 0.21$ nN) (Fig. 13 *g*). Histograms for intermediate ionic strengths lie in between, corresponding to the ionic strength concentrations shown in Fig. 13, *b* and *c*.

CONCLUSIONS

We report on a detailed experimental quantitative force spectroscopy study on how ion binding affects model PC lipid membrane nanomechanics. We have experimentally proved that the higher the ionic strength, the higher the force that must be applied with the AFM tip to penetrate the bilayer. These results are in agreement with recent works that have demonstrated both experimentally and theoretically that cations (both monovalent, e.g., Na^+, and divalent, e.g., Ca^{2+}) penetrate the headgroups of phospholipid molecules, giving rise to a more packed phospholipid network and a higher phospholipid-phospholipid lateral interaction. This increase in lateral interaction between neighboring molecules may be the cause for the extension of the elastic deformation region in the force plots before the plastic region begins (yield threshold force value). An elastic spring model that accounts for lateral

interactions has been proved to fit the experimental deformation data. Moreover, we have extended this work to a natural lipid bilayer (*E. coli* lipid extract), and the same tendency was observed for the force needed to puncture the bilayer to increase with ionic strength. We provide proof that the binding process is fully reversible and we can estimate directly the kinetics of the membrane response through force spectroscopy measurements. In addition, preliminary results concerning the relationship between nanomechanical response and chemical composition of the hydrophobic tail have been shown. This work introduces a new investigation line dealing with the relationship between the experimental measurements regarding the nanomechanics of membranes in the nanometer/nanonewton range and the atomic underlying processes. This is an interesting example of how small variations in chemical composition both in chemical structure and in the surrounding media can translate into considerable variations in the nanomechanical response of the membrane system.

The authors thank the Departament d'Universitats, Recerca i Societat de la Informació (Generalitat de Catalunya) for a grant (S.G.-M.) and for financial support through projects 2000SGR017 and AGP99-10. We thank Dr. Pau Gorostiza for helpful discussions, Dr. S. Vinzelberg (Asylum Research) for software development, and Dr. T. Missana, Centro de Investigaciones Energéticas Medioambientales y Tecnológicas (Madrid) for kindly allowing us to use the Zetamaster equipment.

REFERENCES

1. Cevc, G. 1990. Membrane electrostatics. *Biochim. Biophys. Acta.* 1031:311–382.
2. Binder, H., and O. Zschornig. 2002. The effect of metal cations on the phase behavior and hydration characteristics of phospholipid membranes. *Chem. Phys. Lipids.* 115:39–61.
3. Ohki, S., N. Duzgunes, and K. Leonards. 1982. Phospholipid vesicle aggregation: effect of monovalent and divalent ions. *Biochemistry.* 21:2127–2133.
4. Ohki, S., S. Roy, H. Ohshima, and K. Leonards. 1984. Monovalent cation-induced phospholipid vesicle aggregation: effect of ion binding. *Biochemistry.* 23:6126–6132.
5. Eisenberg, M., T. Gresalfi, T. Riccio, and S. McLaughlin. 1979. Adsorption of monovalent cations to bilayer membranes containing negative phospholipids. *Biochemistry.* 18:5213–5223.
6. Makino, K., T. Yamada, M. Kimura, T. Oka, H. Ohshima, and T. Kondo. 1991. Temperature- and ionic strength-induced conformational changes in the lipid head group region of liposomes as suggested by zeta potential data. *Biophys. Chem.* 41:175–183.
7. Pandit, S. A., D. Bostick, and M. L. Berkowitz. 2003. Molecular dynamics simulation of a dipalmitoylphosphatidylcholine bilayer with NaCl. *Biophys. J.* 84:3743–3750.
8. Pandit, S. A., D. Bostick, and M. L. Berkowitz. 2003. Mixed bilayer containing dipalmitoylphosphatidylcholine and dipalmitoylphosphatidylserine: lipid complexation, ion binding, and electrostatics. *Biophys. J.* 85:3120–3131.
9. Bockmann, R. A., A. Hac, T. Heimburg, and H. Grubmuller. 2003. Effect of sodium chloride on a lipid bilayer. *Biophys. J.* 85:1647–1655.
10. Leonenko, Z. V., A. Carnini, and D. T. Cramb. 2000. Supported planar bilayer formation by vesicle fusion: the interaction of phospholipid vesicles with surfaces and the effect of gramicidin on bilayer properties using atomic force microscopy. *Biochim. Biophys. Acta.* 1509:131–147.
11. Benz, M., T. Gutsmann, N. Chen, R. Tadmor, and J. Israelachvili. 2004. Correlation of AFM and SFA measurements concerning the stability of supported lipid bilayers. *Biophys. J.* 86:870–879.
12. Mueller, H., H. J. Butt, and E. Bamberg. 2000. Adsorption of membrane-associated proteins to lipid bilayers studied with an atomic force microscope: myelin basic protein and cytochrome c. *J. Phys. Chem. B.* 104:4552–4559.
13. Desmeules, P., M. Grandbois, V. A. Bondarenko, A. Yamazaki, and C. Salesse. 2002. Measurement of membrane binding between recoverin, a calcium-myristoyl switch protein, and lipid bilayers by AFM-based force spectroscopy. *Biophys. J.* 82:3343–3350.
14. Kaasgaard, T., C. Leidy, J. H. Ipsen, O. G. Mouritsen, and K. Jorgensen. 2001. In situ atomic force microscope imaging of supported lipid bilayers. *Single Molecules.* 2:105–108.
15. Slade, A., J. Luh, S. Ho, and C. M. Yip. 2002. Single molecule imaging of supported planar lipid bilayer-reconstituted human insulin receptors by in situ scanning probe microscopy. *J. Struct. Biol.* 137:283–291.
16. Schneider, J., W. Barger, and G. U. Lee. 2003. Nanometer scale surface properties of supported lipid bilayers measured with hydrophobic and hydrophilic atomic force microscope probes. *Langmuir.* 19:1899–1907.
17. Seantier, B., C. Breffa, O. Felix, and G. Decher. 2004. In situ investigations of the formation of mixed supported lipid bilayers close to the phase transition temperature. *Nano Lett.* 4:5–10.
18. Corcoran, S. G., R. J. Colton, E. T. Lilleodden, and W. W. Gerberich. 1997. Anomalous plastic deformation at surfaces: nanoindentation of gold single crystals. *Phys. Rev. B.* 55:16057–16060.
19. Fraxedas, J., S. Garcia-Manyes, P. Gorostiza, and F. Sanz. 2002. Nanoindentation: toward the sensing of atomic interactions. *Proc. Natl. Acad. Sci. USA.* 99:5228–5232.
20. Ikai, A., and R. Afrin. 2003. Toward mechanical manipulations of cell membranes and membrane proteins using an atomic force microscope: an invited review. *Cell Biochem. Biophys.* 39:257–277.
21. Franz, V., and H. J. Butt. 2002. Confined liquids: solvation forces in liquid alcohols between solid surfaces. *J. Phys. Chem. B.* 106:1703–1708.
22. O'Shea, S. J., and M. E. Welland. 1998. Atomic force microscopy at solid-liquid interfaces. *Langmuir.* 14:4186–4197.
23. Vezenov, D. V., A. Noy, L. F. Rozsnyai, and C. M. Lieber. 1997. Force titrations and ionization state sensitive imaging of functional groups in aqueous solutions by chemical force microscopy. *J. Am. Chem. Soc.* 119:2006–2015.
24. Ahimou, F., F. A. Denis, A. Touhami, and Y. F. Dufrene. 2002. Probing microbial cell surface charges by atomic force microscopy. *Langmuir.* 18:9937–9941.
25. Rief, M., M. Gautel, F. Oesterhelt, J. M. Fernandez, and H. E. Gaub. 1997. Reversible unfolding of individual titin immunoglobulin domains by AFM. *Science.* 276:1109–1112.
26. Schlierf, M., H. Li, and J. M. Fernandez. 2004. The unfolding kinetics of ubiquitin captured with single-molecule force-clamp techniques. *Proc. Natl. Acad. Sci. USA.* 101:7299–7304.
27. Dufrene, Y. F., T. Boland, J. W. Schneider, W. R. Barger, and G. U. Lee. 1998. Characterization of the physical properties of model biomembranes at the nanometer scale with the atomic force microscope. *Faraday Discuss.* 111:79–94.
28. Richter, R. P., and A. Brisson. 2003. Characterization of lipid bilayers and protein assemblies supported on rough surfaces by atomic force microscopy. *Langmuir.* 19:1632–1640.
29. Franz, V., S. Loi, H. Muller, E. Bamberg, and H. H. Butt. 2002. Tip penetration through lipid bilayers in atomic force microscopy. *Colloids Surf. B Biointerfaces.* 23:191–200.
30. Leonenko, Z. V., E. Finot, H. Ma, T. E. Dahms, and D. T. Cramb. 2004. Investigation of temperature-induced phase transitions in DOPC and DPPC phospholipid bilayers using temperature-controlled scanning force microscopy. *Biophys. J.* 86:3783–3793.

31. Loi, S., G. Sun, V. Franz, and H. J. Butt. 2002. Rupture of molecular thin films observed in atomic force microscopy. II. Experiment. *Phys. Rev. E*: 66:031602/1–031602/7.

32. Butt, H. J., and V. Franz. 2002. Rupture of molecular thin films observed in atomic force microscopy. I. Theory. *Phys. Rev. E.* 66: 031601/1–031601/9.

33. Thompson, J. B., J. H. Kindt, B. Drake, H. G. Hansma, D. E. Morse, and P. K. Hansma. 2001. Bone indentation recovery time correlates with bond reforming time. *Nature*. 414:773–776.

34. Ratanabanangkoon, P., and A. P. Gast. 2003. Effect of ionic strength on two-dimensional streptavidin crystallization. *Langmuir*. 19:1794–1801.

35. Bockmann, R. A., and H. Grubmuller. 2004. Multistep binding of divalent cations to phospholipid bilayers: a molecular dynamics study. *Angew. Chem. Int. Ed. Engl.* 43:1021–1024.

36. Newman, M. J., and T. H. Wilson. 1980. Solubilization and reconstitution of the lactose transport system from Escherichia coli. *J. Biol. Chem.* 255:10583–10586.

37. Florin, E. L., M. Rief, H. Lehmann, M. Ludwig, C. Dornmair, V. T. Moy, and H. E. Gaub. 1995. Sensing specific molecular interactions with the atomic force microscope. *Biosens. Bioelectron.* 10:895–901.

38. Proksch, R., T. E. Schaffer, J. P. Cleveland, R. C. Callahan, and M. B. Viani. 2004. Finite optical spot size and position corrections in thermal spring constant calibration. *Nanotechnology.* 15:1344–1350.

39. Yang, J., and J. Appleyard. 2000. The main phase transition of mica-supported phosphatidylcholine membranes. *J. Phys. Chem. B*. 104: 8097–8100.

40. Egawa, H., and K. Furusawa. 1999. Liposome adhesion on mica surface studied by atomic force microscopy. *Langmuir.* 15:1660–1666.

41. Silin, V. I., H. Wieder, J. T. Woodward, G. Valincius, A. Offenhausser, and A. L. Plant. 2002. The role of surface free energy on the formation of hybrid bilayer membranes. *J. Am. Chem. Soc.* 124:14676–14683.

42. Pera, I., R. Stark, M. Kappl, H. J. Butt, and F. Benfenati. 2004. Using the atomic force microscope to study the interaction between two solid supported lipid bilayers and the influence of synapsin I. *Biophys. J.* 87:2446–2455.

43. Butt, H. J. 1991. Electrostatic interaction in atomic force microscopy. *Biophys. J.* 60:777–785.

44. Pasenkiewicz-Gierula, M., Y. Takaoka, H. Miyagawa, K. Kitamura, and A. Kusumi. 1997. Hydrogen bonding of water to phosphatidylcholine in the membrane as studied by a molecular dynamics simulation: location, geometry, and lipid-lipid bridging via hydrogen-bonded water. *J. Phys. Chem. A.* 101:3677–3691.

45. Pasenkiewicz-Gierula, M., Y. Takaoka, H. Miyagawa, K. Kitamura, and A. Kusumi. 1999. Charge pairing of headgroups in phosphatidylcholine membranes: a molecular dynamics simulation study. *Biophys. J.* 76:1228–1240.

46. Israelachvili, J. 1991. Intermolecular and Surface Forces. Academic Press, London.

47. Marra, J., and J. Israelachvili. 1985. Direct measurements of forces between phosphatidylcholine and phosphatidylethanolamine bilayers in aqueous electrolyte solutions. *Biochemistry.* 24:4608–4618.

48. Tristram-Nagle, S., Y. Liu, J. Legleiter, and J. F. Nagle. 2002. Structure of gel phase DMPC determined by x-ray diffraction. *Biophys. J.* 83:3324–3335.

49. Ho, C., and C. D. Stubbs. 1997. Effect of n-alkanols on lipid bilayer hydration. *Biochemistry.* 36:10630–10637.

50. Johnson, K. L. 1985. Contact Mechanics. Cambridge University Press, Cambridge, UK.

51. Pandit, S. A., and M. L. Berkowitz. 2002. Molecular dynamics simulation of dipalmitoylphosphatidylserine bilayer with Na+ counterions. *Biophys. J.* 82:1818–1827.